

KFKI-1981-82

M.A. SZUHAR

COMPUTATION OF IDEAL C-V CURVES FOR
NONUNIFORMLY DOPED MOS STRUCTURES

Hungarian Academy of Sciences

CENTRAL
RESEARCH
INSTITUTE FOR
PHYSICS

BUDAPEST

COMPUTATION OF IDEAL C-V CURVES FOR NONUNIFORMLY DOPED MOS STRUCTURES

M.A. Szuhar

Central Research Institute for Physics
H-1525 Budapest 114, P.O.B. 49, Hungary

HU ISSN 0368 5330
ISBN 963 371 864 3

ABSTRACT

A simple one-dimensional numerical simulation technique is proposed as a means of solving the Poisson equation applied for MOS capacitances with arbitrary doping profile. The discontinuity condition valid at the Si-SiO₂ interface was built into the governing equation system enabling accurate solution for potential and charge distributions. Based on the accurate solutions ideal C-V curves were derived whose validity was proved by comparing them with the curves obtained from the exact solution in the special uniform case. The computer program is verified by ideal C-V curves given for enhancement and for depletion type ion-implanted MOS structures.

АННОТАЦИЯ

В статье дается решение уравнения Пуассона в одномерном пространстве с целью математического моделирования МОП диодов с неоднородным распределением примесей. Применением справедливой на границе раздела фаз Si-SiO₂ теоремы Гаусса в уравнении Пуассона, функции распределения электростатического потенциала и концентрации электронов и дырок решаются с необходимой точностью. На основе этих результатов определяется идеальная C-V характеристика МОП диодов. Точность цифровых расчетов доказывается сравнением результатов расчетов с результатами, полученными в явном виде для случая однородного распределения примесей, а для демонстрации широкой применимости вычислительной программы даются идеальные C-V характеристики, определенные в случае МОП диодов с неоднородным распределением примесей.

KIVONAT

A dolgozat az egydimenziós Poisson egyenlet megoldásán keresztül tetszőleges adalék eloszlású MOS kapacitások szimulációját írja le. A Si-SiO₂ határfelületen érvényesülő Gauss tétel Poisson egyenletbe építésével a potenciál és töltéseloszlásra megfelelő pontosságú eredményt kaptunk. A potenciál és töltéseloszlás ismeretében pedig meghatároztuk MOS kapacitások ideális C-V görbéit. A numerikus eljárás pontosságának igazolására a homogén adalékeloszlás esetén kapott numerikus eredményeinket összehasonlítottuk az ebben az esetben nyerhető exact megoldással. Továbbá, a számítógép program széles körű alkalmazhatóságának bizonyítására megadtuk az ideális C-V görbéjét egy növekvő és egy kiürítési ion-implantált MOS kapacitásnak.

NOTATION

C	low frequency MOS capacitance per unit area ($F\text{ cm}^{-2}$)
C_{ox}	oxide capacitance per unit area ($F\text{ cm}^{-2}$)
C_{si}	low frequency differential semiconductor capacitance per unit area ($F\text{ cm}^{-2}$)
DOP (x)	impurity distribution (cm^{-3})
DOPN (x)	impurity distribution in dimensionless form
d_{ox}	oxide thickness (cm)
D_{ox}	oxide thickness in dimensionless form
h	mesh spacing in dimensionless form
l	length of the examined sample (cm)
L	length of the examined sample in dimensionless form
N	number of grid points
N_{A}	acceptor concentration (cm^{-3})
N_{D}	donor concentration (cm^{-3})
N_{O}	implanted dose (cm^{-3})
n_{i}	intrinsic carrier concentration (cm^{-3})
q	magnitude of electronic charge (A s)
Q	charge per unit square ($A\text{ s cm}^{-2}$)
R_{p}	projected range (cm)
s	the number of the surface point
V	electrostatic potential in dimensionless form
V_{B}	bulk potential (V)
V_{G}	gate potential (V)
V_{S}	surface potential in dimensionless form
x	coordinate, distance measured from the gate contact (cm)
X	coordinate in dimensionless form
ϵ_{ox}	dielectric constant of the oxide
ϵ_{si}	dielectric constant of the silicon
ϕ_{n}	quasi-Fermi potential for electrons (V)
ϕ_{p}	quasi-Fermi potential for holes (V)
ϕ_{T}	thermal voltage (V)
ψ	electrostatic potential (V)
ρ	space charge density ($A\text{ s cm}^{-3}$)
δ	standard deviation of the implanted layer (cm)

NOTATION

a	the frequency of the signal
b	the frequency of the noise
c	the frequency of the carrier
d	the frequency of the modulator
e	the frequency of the demodulator
f	the frequency of the filter
g	the frequency of the amplifier
h	the frequency of the receiver
i	the frequency of the transmitter
j	the frequency of the antenna
k	the frequency of the antenna
l	the frequency of the antenna
m	the frequency of the antenna
n	the frequency of the antenna
o	the frequency of the antenna
p	the frequency of the antenna
q	the frequency of the antenna
r	the frequency of the antenna
s	the frequency of the antenna
t	the frequency of the antenna
u	the frequency of the antenna
v	the frequency of the antenna
w	the frequency of the antenna
x	the frequency of the antenna
y	the frequency of the antenna
z	the frequency of the antenna
A	the amplitude of the signal
B	the amplitude of the noise
C	the amplitude of the carrier
D	the amplitude of the modulator
E	the amplitude of the demodulator
F	the amplitude of the filter
G	the amplitude of the amplifier
H	the amplitude of the receiver
I	the amplitude of the transmitter
J	the amplitude of the antenna
K	the amplitude of the antenna
L	the amplitude of the antenna
M	the amplitude of the antenna
N	the amplitude of the antenna
O	the amplitude of the antenna
P	the amplitude of the antenna
Q	the amplitude of the antenna
R	the amplitude of the antenna
S	the amplitude of the antenna
T	the amplitude of the antenna
U	the amplitude of the antenna
V	the amplitude of the antenna
W	the amplitude of the antenna
X	the amplitude of the antenna
Y	the amplitude of the antenna
Z	the amplitude of the antenna
A	the amplitude of the antenna
B	the amplitude of the antenna
C	the amplitude of the antenna
D	the amplitude of the antenna
E	the amplitude of the antenna
F	the amplitude of the antenna
G	the amplitude of the antenna
H	the amplitude of the antenna
I	the amplitude of the antenna
J	the amplitude of the antenna
K	the amplitude of the antenna
L	the amplitude of the antenna
M	the amplitude of the antenna
N	the amplitude of the antenna
O	the amplitude of the antenna
P	the amplitude of the antenna
Q	the amplitude of the antenna
R	the amplitude of the antenna
S	the amplitude of the antenna
T	the amplitude of the antenna
U	the amplitude of the antenna
V	the amplitude of the antenna
W	the amplitude of the antenna
X	the amplitude of the antenna
Y	the amplitude of the antenna
Z	the amplitude of the antenna

1. INTRODUCTION

With the appearance of large scale integration and new, sophisticated semiconductor technologies the significance of the MOS technique has increased faster than ever. The rapid development in this field demands more accurate and flexible methods for designing and measuring MOS structures. The well-known C-V technique, for example, which is widely used for process control or as a design tool [1], has preserved its significance but the evaluation of the desired parameters from it has become much more difficult and inaccurate mainly due to the nonuniform doping level near the Si-SiO₂ interface.

Such nonuniform doping level can be created intentionally by shallow diffusion or ion implantation so that the threshold voltage can be adjusted, but this may also occur unavoidably due to the redistribution of dopants during thermal oxidation.

Moreover, if the doping level near the interface is nonuniform, the Poisson equation, describing the potential distribution in the MOS structure cannot be solved exactly and the well-known ideal curves of Goetzberger [2] based on the exact solution for the uniform case [3] cannot be used in the evaluation, what means the Poisson equation should be solved numerically.

However a difficulty arises during the numerical computation due to the heterogeneous structure studied, since an intermediate boundary exists at the Si - SiO₂ interface, where the space charge and the dielectric constant are discontinuous. The discontinuity of these functions could be handled by the box integration technique described with mathematical rigour in [4] and utilized among others in [5], since the required conditions are fulfilled, but it would result in a fictitious surface charge violating Gauss's law. Though this fictitious surface charge can even partially compensate the error of the numerical differentiation at low values of space charge using fine mesh spacings near the surface, but it causes unacceptable error at high values of surface space charge.

The purpose of the present paper is to overcome this problem and to introduce a sufficiently accurate and effective one-dimensional mathematical model suitable for deriving ideal C-V curves for MOS capacitances with arbitrary doping profile allowing, at the same time, the presence of a p-n

junction, too. On the basis of this mathematical model the dependence of the C-V characteristics on the parameters of the doping profile and on the other properties of the MOS structure might be given, but the number of required graphical plots would be unreasonable. It is for this reason that we wish only to verify the accuracy of the mathematical model by comparing the C-V curves derived in this way with the ideal curves of Goetzberger [2] at uniform doping, and to give only two examples for the solution of the nonuniform case - together of course with a detailed description of the applied numerical technique.

2. MODEL FORMULATION

If it is assumed that the examined MOS capacitance has a sufficiently large area for the side effects to have no influence on the field chosen for simulation and the doping level is nonuniform only in the direction normal to the interface, then the problem can be accepted as one-dimensional. In this case the governing Poisson equation can be written, as follows:

$$\frac{d^2\psi}{dx^2} = - \frac{\rho}{\epsilon} \quad (1)$$

However as was stated earlier the right hand side function of this equation is discontinuous at the Si - SiO₂ interface resulting in an undifferentiable electrostatic potential at this particular point. Therefore it seems to be reasonable to divide the Poisson equation and use it separately for the oxide and for the semiconductor area connecting them only through the Gauss's law determining the potential at the interface and ensuring internal boundary conditions for the two separated Poisson equations. This way the generation of some fictitious space charge, violating the Gauss's law and created unavoidably at box integration is avoided.

Since we are concerned here with ideal MOS capacitance the oxide charge, the interface states and the metal-semiconductor work function difference are to be neglected, though taking into account these parameters at the Gauss's law would not cause any mathematical problem.

Corresponding to all that has been stated the governing differential equation system can be written, as:

$$\begin{aligned} \frac{d^2\psi}{dx^2} &= 0 && \text{if } 0 \leq x < d_{\text{ox}} \\ \epsilon_{\text{ox}} \left. \frac{d\psi}{dx} \right|_{x=d_{\text{ox}}^-} &= \epsilon_{\text{si}} \left. \frac{d\psi}{dx} \right|_{x=d_{\text{ox}}^+} && \text{if } x = d_{\text{ox}} \end{aligned} \quad (2)$$

$$\frac{d^2\psi}{dx^2} = - \frac{\rho}{\epsilon_{si}} \quad \text{if } x > d_{ox}$$

with the boundary conditions:

$$\psi(0) = V_G$$

$$\psi(\ell) = V_B$$

where ℓ is a long enough distance from the gate contact to ensure that the boundary point $x = \ell$ is in the neutral region of the bulk.

The space charge in the silicon can be described by:

$$\rho = q \cdot [n_i \cdot \phi_n \cdot \exp(\psi/\phi_T) - n_i \cdot \phi_p \cdot \exp(-\psi/\phi_T) - \text{DOP}] \quad (3)$$

where:

$$\phi_n = \exp(-\phi_n/\phi_T)$$

$$\phi_p = \exp(\phi_p/\phi_T) \quad (4)$$

$$\text{DOP} = \begin{cases} - N_A & \text{for p - type silicon} \\ N_D & \text{for n - type silicon} \end{cases}$$

The presence of the exponential quasi-Fermi potentials, as variables, will not cause any problem, because the current density in an ideal MOS capacitance at steady state is zero and accordingly the quasi-Fermi potentials will be equal and constant throughout the silicon. For simplicity, it is reasonable to take $\phi_n = \phi_p = 0$ causing $\phi_n = \phi_p = 1$; this naturally means that all the potentials from now on should be related to this reference point.

For convenience, in the numerical calculations, the normalized forms of the variables will be used, i.e. the distances will be in units of Debye length, the potentials and voltages in units of thermal voltage, the field charge in units of electron charge and the charge and impurity concentrations in units of intrinsic concentration. Though it could be handled in another way, too the relative dielectric constants were included in the Debye length, resulting in different normalization factors for distances in the oxide and in the silicon.

If we utilize these simplifications the differential equation system used for the numerical calculations will be:

$$\frac{d^2V}{dx^2} = 0 \quad \text{if } 0 \leq X < D_{OX}$$

$$\left. \frac{dV}{dx} \right|_{X=D_{OX}^-} = (\epsilon_{si}/\epsilon_{ox})^{1/2} \left. \frac{dV}{dx} \right|_{X=D_{OX}^+} \quad \text{if } X=D_{OX} \quad (5)$$

$$\frac{d^2V}{dx^2} = \exp(V) - \exp(-V) - DOPN \quad \text{if } X > D_{OX}$$

$$V(0) = V_G/\phi_T$$

$$V(L) = V_G/\phi_T$$

To avoid difficulties with transcendental equations (5) was linearized in the most general way [6], i.e. by substituting V with another variable $\delta = V_{NEW} - V_{OLD}$ and using Taylor series expansion in the vicinity of V_{OLD} for the exponential terms. Here V_{OLD} is an intermediate or trial solution accepted as known in an iteration cycle and V_{NEW} is the solution based on it, what means that δ is the error between two successive iteration steps approaching zero at a converging procedure.

This transforms equation (5) into:

$$\frac{d^2\delta}{dx^2} = - \frac{d^2V_{OLD}}{dx^2} \quad \text{if } 0 \leq X < D_{OX} \quad (6)$$

$$(\epsilon_{si}/\epsilon_{ox})^{1/2} \left. \frac{d\delta}{dx} \right|_{X=D_{OX}^+} - \left. \frac{d\delta}{dx} \right|_{X=D_{OX}^-} = \left. \frac{dV_{OLD}}{dx} \right|_{X=D_{OX}^-}$$

$$- (\epsilon_{si}/\epsilon_{ox})^{1/2} \left. \frac{dV_{OLD}}{dx} \right|_{X=D_{OX}^+} \quad \text{if } X=D_{OX}$$

$$\frac{d^2\delta}{dx^2} - [\exp(V_{OLD}) + \exp(-V_{OLD})] \cdot \delta =$$

$$= - \frac{d^2V_{OLD}}{dx^2} + \exp(V_{OLD}) - \exp(-V_{OLD}) - DOPN \quad \text{if } X > D_{OX}$$

with the appropriate boundary conditions:

$$\delta(0) = 0 \quad V_{OLD} = V_{NEW} = V_G/\phi_T$$

$$\delta(L) = 0 \quad V_{OLD} = V_{NEW} = V_B/\phi_T$$

3. NUMERICAL TECHNIQUE

Equation system (6), already suitable for numerical calculation, was discretized by the traditional three-point finite difference scheme [4], resulting in a linear equation system based on a three-diagonal sparse matrix. The terms of the matrix and the right-side vector for a general i point in the grid system, corresponding to the i th row of the linear equation system, can be given as follows:

$$\begin{array}{l}
 a_{i,i-1} = 2/h_i (h_i + h_{i+1}) \\
 a_{i,i} = -2/h_i \cdot h_{i+1} \\
 a_{i,i+1} = 2/h_{i+1} (h_i + h_{i+1}) \\
 b_i = -a_{i,i-1} \cdot V_{OLD\ i-1} - a_{i,i} \cdot V_{OLD\ i} - a_{i,i+1} V_{OLD\ i+1}
 \end{array}
 \left. \vphantom{\begin{array}{l} a_{i,i-1} \\ a_{i,i} \\ a_{i,i+1} \\ b_i \end{array}} \right\} \text{if } 0 \leq X < D_{Ox}$$

$$\begin{array}{l}
 a_{i,i-1} = 0,57/h_i \\
 a_{i,i+1} = 1/h_{i+1} \\
 a_{i,i} = -a_{i,i-1} - a_{i,i+1} \\
 b_i = -a_{i,i-1} \cdot V_{OLD\ i-1} - a_{i,i} \cdot V_{OLD\ i} - a_{i,i+1} \cdot V_{OLD\ i+1}
 \end{array}
 \left. \vphantom{\begin{array}{l} a_{i,i-1} \\ a_{i,i+1} \\ a_{i,i} \\ b_i \end{array}} \right\} \text{if } X = D_{Ox}$$

$$\begin{array}{l}
 a_{i,i-1} = 2/h_i (h_i + h_{i+1}) \\
 a_{i,i} = -2/h_i h_{i+1} \exp(V_{OLD\ i}) - \exp(-V_{OLD\ i}) \\
 a_{i,i+1} = 2/h_{i+1} (h_i + h_{i+1}) \\
 b_i = -a_{i,i-1} V_{OLD\ i-1} - a_{i,i} V_{OLD\ i} - a_{i,i+1} V_{OLD\ i+1} + \\
 \quad + \exp(V_{OLD\ i}) - \exp(-V_{OLD\ i}) - DOPN_i
 \end{array}
 \left. \vphantom{\begin{array}{l} a_{i,i-1} \\ a_{i,i} \\ a_{i,i+1} \\ b_i \end{array}} \right\} \text{if } D_{Ox} < X \leq L$$

At this step an assumption was made, viz. that the field strength is constant between the interface and the grid point next to the interface and the value of it corresponds to the exact value just at the silicon side of the interface. This assumption coincides with the reality at the oxide side and causes an acceptable error at reasonable grid system in the silicon. Naturally, if using of a coarse grid system is unavoidable, the field strength at the silicon side is to be approached through a more accurate finite difference formulation.

It is easy to realize that the matrix of the created linear equation system, including the discretized Gauss's law will be diagonally dominant and positive definite, thereby ensuring the convergence of the iterative solution processes. There is no reason to use a direct solution technique such as Gauss elimination because this would permit error truncation and fill the sparse matrix with undesirable terms rapidly increasing the required store capacity. The use of sophisticated iterative techniques, like block iteration or strongly implicit procedure, also seems to be unreasonable because the much simpler and convenient successive over - relaxation SOR method [4] with appropriate acceleration factor ensures a very good convergence. Thus, the mentioned SOR procedure was applied for the solution of the linear equation system with an $\omega=1.73$ acceleration factor. The solution was truncated when the maximum charge in δ was less than 10%. The linear equation system was modified on the basis of the new intermediate solution, V_{NEW} , creating in this way an outer cycle for the solution of the electrostatic potential, V . The rate of convergence could be improved by applying an acceleration factor in the outer cycle, too. But, when it is used during the initial stages of the outer loop instabilities could occur. The outer cycle was stopped when the absolute maximum value of δ decreased below 10^{-4} , i.e. when the electrostatic potential at every point of the grid system was known with less than $\pm 2.6\mu V$ error.

Further on the silicon capacitance can be defined as the slope of charge change caused by the surface potential perturbation. That is,

$$C_{Si} = \frac{\partial Q}{\partial \psi_s} \quad (8)$$

This can be written in numerical form, using the previous simplifications, as:

$$C_{Si} = a \frac{\sum_{i=s}^N [\exp(V_i^{k+1}) - \exp(V_i^k) + \exp(-V_i^k) - \exp(-V_i^{k+1})] \cdot h_i}{V_s^{k+1} - V_s^k} \quad (9)$$

Here "a" is a constant used to transform the dimensionless form into SI one and the k and k+1 suffixes refer to the two different potential distributions obtained at V_G and $V_G + \Delta$ gate voltages, where Δ is a sufficiently small voltage change. The value of a equals $3,14 \cdot 10^{-10}$ F/cm² for silicon at $T=300^\circ K$ assuming that the described normalization technique was applied for the numerical calculation of the potential distribution.

With the knowledge of C_{Si} at a given gate voltage the relative capacitance C/C_{Ox} of the MOS structure can be obtained as

$$C/C_{Ox} = \frac{C_{Si}}{\epsilon_{Ox}/d_{Ox} + C_{Si}} \quad (10)$$

If the described numerical calculations are repeated at the desired gate voltages the ideal curves for MOS capacitances with arbitrary profile can be derived.

4. RESULTS

On the basis of the described numerical technique a FORTRAN program was developed suitable for determining the potential and charge distribution in a MOS capacitance and enabling these results to be used to derive the required ideal C-V curve. The distribution of the grid points in the silicon was made in accordance with an error analysis, on which a report was published earlier [7], stating that the potential distance between two neighbouring points should not exceed $10\phi_T$ to ensure an accurate solution. In order to fulfil this requirement and to achieve sufficient accuracy near the interface a 20\AA spacing was chosen next to the interface increasing in accordance with geometrical progression. Applying fifty grid points altogether for deriving the ideal C-V curve by calculating the relative capacitance at 20 different gate voltages, a main store capacity of 42K and less than 120 sec CPU time was required for computation on an ES - 1040 computer even though a very primitive trial solution was used at the starting gate voltage.

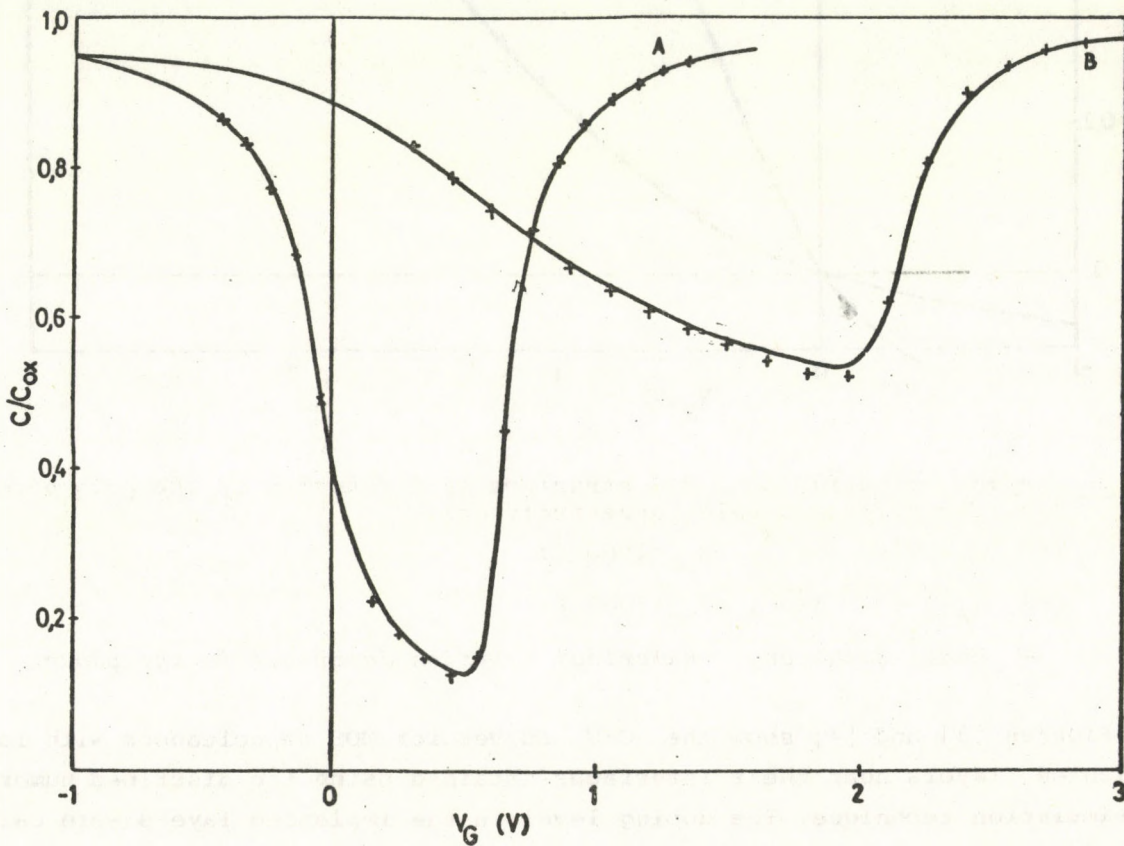


Fig. 1. Low frequency relative MOS capacitance as a function of the gate potential for different bulk concentrations:

(A) $N_A = 1 \cdot 10^{14} \text{ cm}^{-3}$, $d_{ox} = 1000 \text{ \AA}$:

(B) $N_A = 1 \cdot 10^{16} \text{ cm}^{-3}$, $d_{ox} = 1000 \text{ \AA}$:

— exact solution, + numerical solution described in the paper,

Figures 1 and 2 show a comparison of two ideal C-V curves and potential distributions gained by the exact solution of the governing equation for uniform doping with the results obtained from the described numerical simulation procedure to verify the validity and the accuracy of this technique.

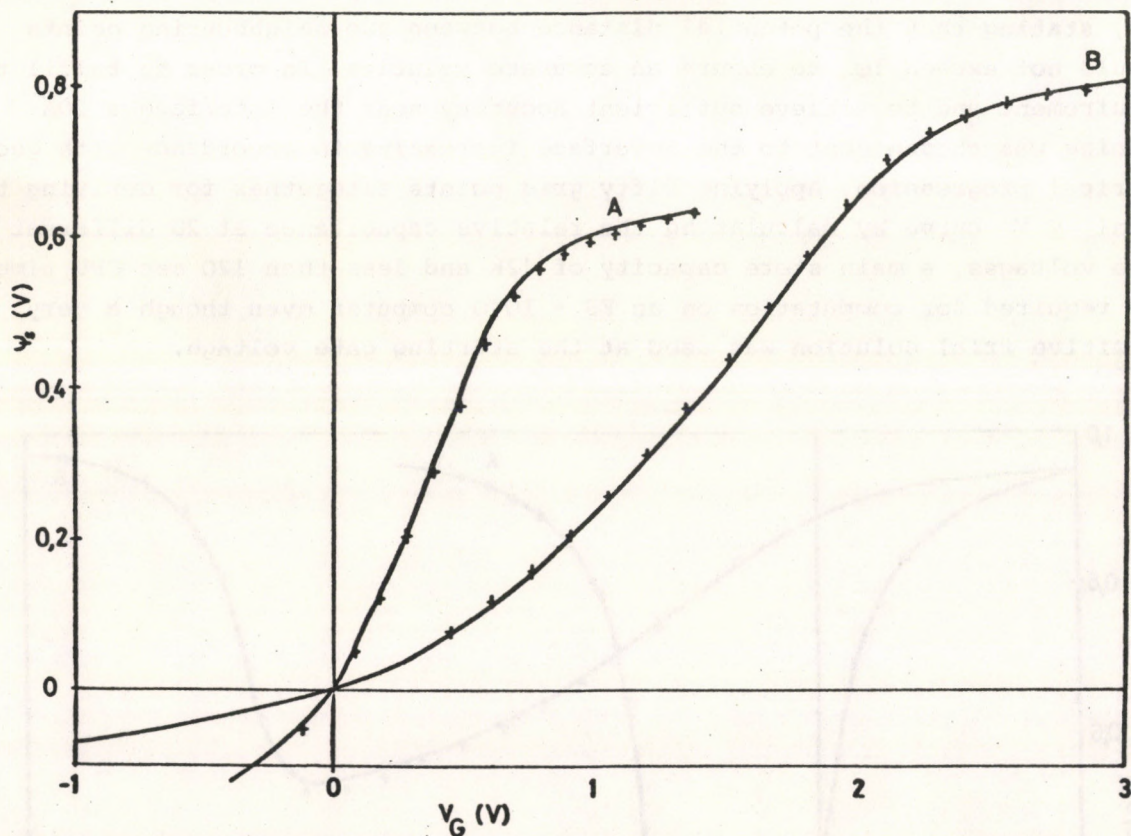


Fig. 2. Surface potential in a MOS structure as a function of the gate potential for different bulk concentrations:

(A) $N_A = 1 \cdot 10^{14} \text{ cm}^{-3}$, $d_{ox} = 1000 \text{ \AA}$:

(B) $N_A = 1 \cdot 10^{16} \text{ cm}^{-3}$, $d_{ox} = 1000 \text{ \AA}$:

— exact solution, + numerical solution described in the paper.

Figures [3] and [4] show the C-V curves for MOS capacitances with ion-implanted layers near their interfaces obtained using the described numerical simulation technique. The doping level in the implanted layers were calculated by means of the normal Gaussian distribution:

$$\text{DOP}_{\text{imp}}(x) = \frac{N_o}{(2\pi\delta^2)^{1/2}} \exp\left[-\frac{(x-R_p)^2}{2\delta^2}\right] \quad (11)$$

This distribution might be changed during heat treatments, but the discussion of this subject is beyond the frame of the present work.

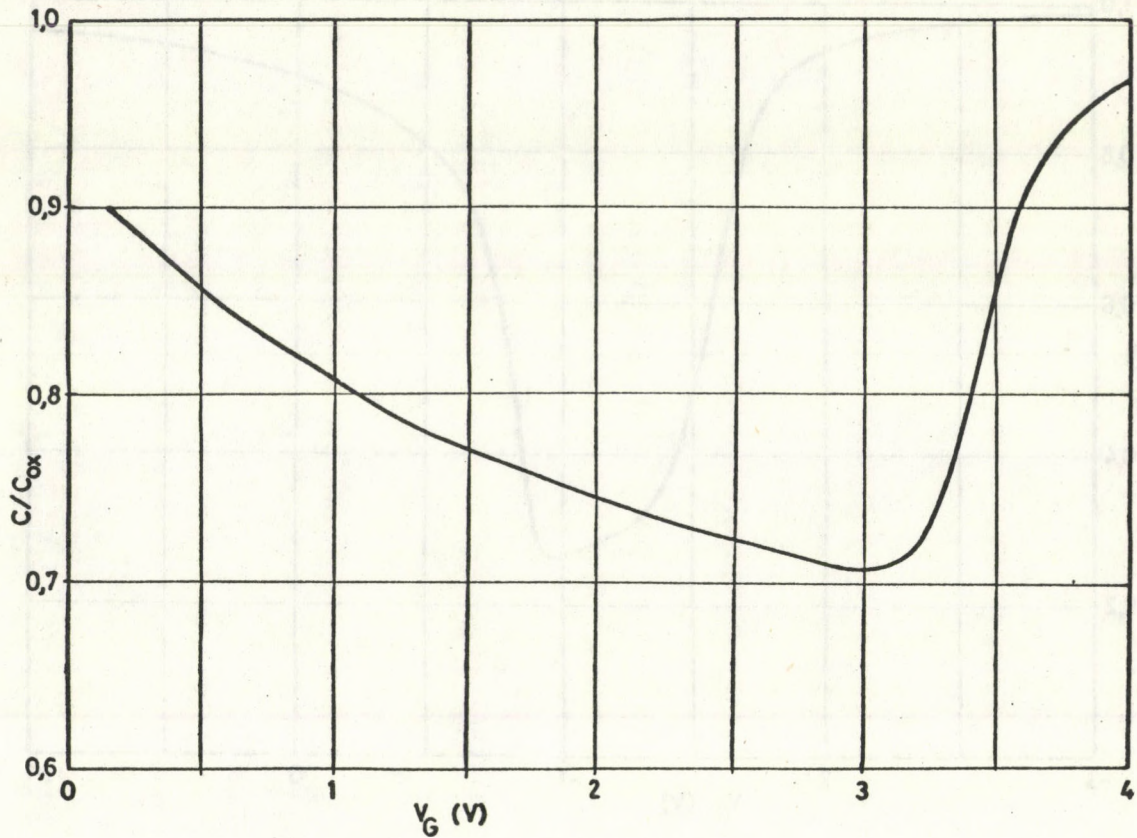


Fig. 3. Low frequency MOS capacitance as a function of the gate potential for an enhancement type implanted MOS structure with the parameters:
 $N_A=1 \cdot 10^{15} \text{ cm}^{-3}$, $N_0=1,25 \cdot 10^{12} \text{ cm}^{-2}$, $R_p=1910 \text{ \AA}$;
 $\delta=550 \text{ \AA}$, $d_{ox}=1000 \text{ \AA}$.

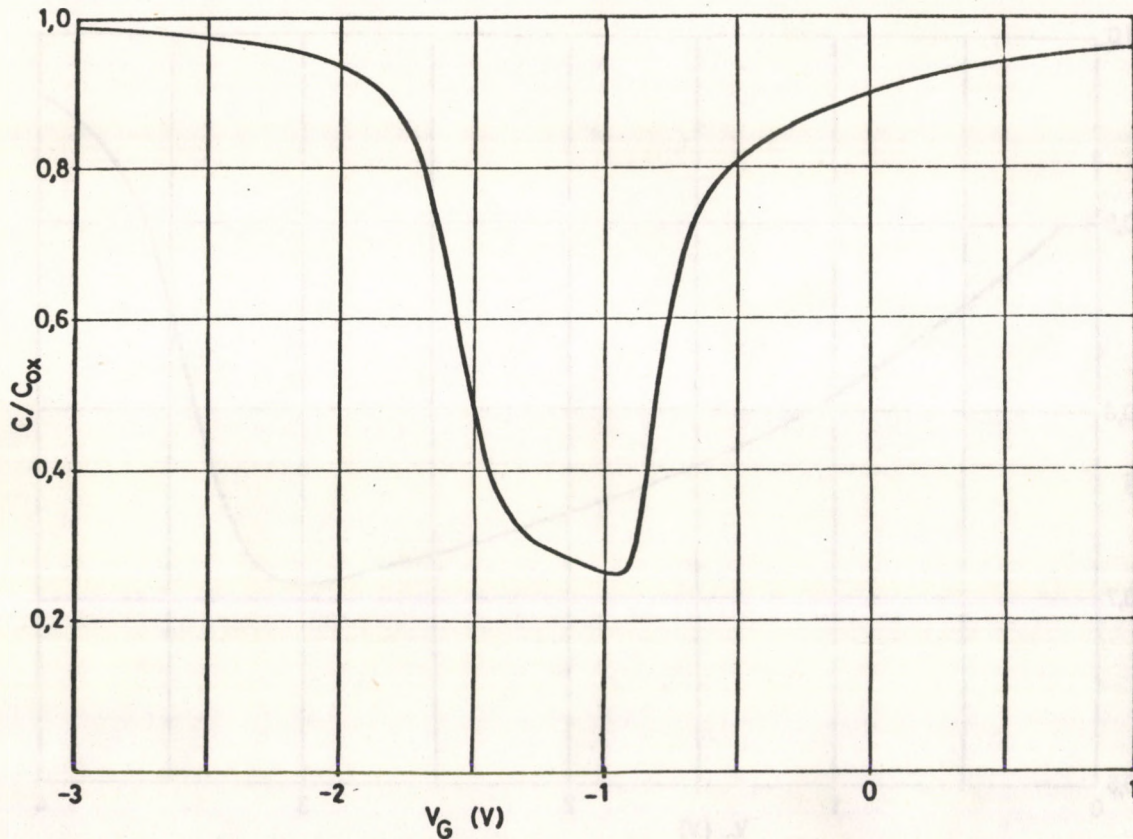


Fig. 4. Low frequency MOS capacitance as a function of the gate voltage for a depletion type implanted MOS structure with the parameters:

$$N_A = 1 \cdot 10^{15} \text{ cm}^{-3}, \quad N_O = 6,25 \cdot 10^{11} \text{ cm}^{-2}, \quad R_p = 1120 \text{ \AA}$$
$$\delta = 400 \text{ \AA}, \quad d_{ox} = 1000 \text{ \AA}.$$

5. CONCLUSION

The proposed model is suitable for deriving ideal C-V curves of MOS capacitances with arbitrary doping profile and contributes to a better understanding of the physical processes taking place in them. The numerical techniques used have proved to be effective and accurate for the solution of this task. Nevertheless, a more accurate method based on measurements or process simulation is required to support this program with the real doping level to make this simulation technique a more effective tool in device design and process control.

ACKNOWLEDGEMENT

The author wishes to thank T. Mohacsy for his critical review of the manuscript.

REFERENCES

- [1] K.H. Zaininger, F.P. Heiman: The C-V technique as an analytical tool, Solid-State Technology 1970. Vol. 5.pp. 49-56
- [2] A. Goetzberger: Ideal MOS curves, Bell System Technical Journal, 1966. Vol. 45.pp. 1097-1122
- [3] S.M. Sze: Physics of semiconductor devices, Wiley, New York, 1969
- [4] R.S. Varga: Matrix iterative analysis, Prentice-Hall, New York, 1962
- [5] F.de la Moneda: Threshold voltage from numerical solution of the two-dimensional MOS transistor, IEEE Trans. Circuit Theory, 1973. Vol. CT-20 pp. 666-674
- [6] H.K. Gummel: Selfconsistent iterative scheme for one-dimensional steady state transistor calculations, IEEE Trans. Electron Devices, 1964. Vol. ED-11 pp. 455-465
- [7] M.A. Szuhár: Two-dimensional MOS transistor simulation, 1981. KFKI report, KFKI-1981-13.





Kiadja a Központi Fizikai Kutató Intézet
Felelős kiadó: Krén Emil
Szakmai lektor: Mohácsi Tibor
Nyelvi lektor: Harvey Shenker
Gépelte: Balczer Györgyné
Példányszám: 465 Törzsszám: 81-571
Készült a KFKI sokszorosító üzemében
Felelős vezető: Nagy Károly
Budapest, 1981. október hó